

# Proton Threshold States in the $^{22}\text{Na}(p, \gamma)^{23}\text{Mg}$ Reaction and Astrophysical Implications

H. Comisel\* and C. Hategan

*Institute of Atomic Physics, Bucharest, PO Box MG-6, Romania*

G. Graw and H.H. Wolter

*Department für Physik, Universität München, D-85748 Garching, Germany*

(Dated: October 31, 2018)

Proton threshold states in  $^{23}\text{Mg}$  are important for the astrophysically relevant proton capture reaction  $^{22}\text{Na}(p, \gamma)^{23}\text{Mg}$ . In the indirect determination of the resonance strength of the lowest states, which were not accessible by direct methods, some of the spin-parity assignments remained experimentally uncertain. We have investigated these states with Shell Model, Coulomb displacement, and Thomas-Ehrman shift calculations. From the comparison of calculated and observed properties we relate the lowest relevant resonance state at  $E_x=7643$  keV to an excited  $3/2^+$  state in accordance with a recent experimental determination by Jenkins *et al.*. From this we deduce significantly improved values for the  $^{22}\text{Na}(p, \gamma)^{23}\text{Mg}$  reaction rate at stellar temperatures below  $T_9=0.1\text{K}$ .

PACS numbers: 25.40.Lw, 21.10.Pc, 21.60.Cs, 97.10.Cv

## I. INTRODUCTION

In nuclear astrophysics the understanding of the *rp* processes as a dominant reaction sequence for the Ne-Na cycle is a topic of current interest. Studies of this cycle also have to explain the anomalous abundance of the  $^{22}\text{Ne}$  isotope observed in the composition of the Orgueil meteorite (called Ne-E; E is for extraordinary) by Black *et al.* in 1972 [1]. This isotope is considered to originate from beta decay of  $^{22}\text{Na}$ . The increased abundance of  $^{22}\text{Ne}$  (with a ratio  $^{22}\text{Ne}/^{20}\text{Ne} \geq 0.67$  much higher than the terrestrial  $^{22}\text{Ne}/^{20}\text{Ne} = 0.1$ ) points to a scenario of considerable production of  $^{22}\text{Na}$  and relatively weak burning of this material in the  $^{22}\text{Na}(p, \gamma)^{23}\text{Mg}$  reaction during the beta decay life time of  $^{22}\text{Na}$  ( $T_{1/2}=2.6$  yr). Sizeable  $^{23}\text{Mg}$  production is expected in the hot Ne-Na cycle, developing in explosive H-burning locations such as novae. The competition between the production and the hydrogen burning of  $^{22}\text{Na}$  in the proton capture reaction  $^{22}\text{Na}(p, \gamma)^{23}\text{Mg}$  has been analyzed in the literature and temperatures defining hot and cold burning modes have been estimated. The astrophysical aspects of the  $^{22}\text{Na}(p, \gamma)^{23}\text{Mg}$  reaction have been outlined in more detail in the work of Seuthe *et al.* [2] and Schmidt *et al.* [3]. The results of the last decade concerning thermonuclear rates for reactions induced by charged particles are systematized in the comprehensive compilation of Angulo *et al.* [4].

The astrophysical calculations of the the stellar reaction rate of the proton capture reaction  $^{22}\text{Na}(p, \gamma)^{23}\text{Mg}$  take into account as many as 21 resonances in  $^{23}\text{Mg}$ . The properties of the lowest three resonances could not be determined by direct measurements because of the

very small capture cross-sections at these low proton energies. Lower and upper limits of the resonance reaction strengths, however, have been determined in an indirect way, using the proton transfer reaction  $^{22}\text{Na}(^{3}\text{He}, d)^{23}\text{Mg}$  [3]. There the energy integrated resonance strengths have been calculated from the spectroscopic factors obtained from the transfer data within the standard DWBA method, and from the single particle resonance widths evaluated from the optical model.

The first resonance, corresponding to the  $E_x=7583$  keV state in  $^{23}\text{Mg}$ , is very close to the proton capture threshold ( $Q_p=7579$  keV [5]) and, by barrier penetration arguments, its contribution to the reaction rate is negligible. The strengths of the next two resonances, the  $E_x=7622$  and  $7643$  keV levels, were evaluated to be within the limits  $5.6 \times 10^{-14} \leq \omega\gamma \leq 8.8 \times 10^{-12}$  meV and  $1.2 \times 10^{-10} \leq \omega\gamma \leq 3.1 \times 10^{-8}$  meV, respectively [3]. Thus for the reaction rates at stellar temperatures below  $T_9 = 0.1$  the third resonance at  $E_x=7643$  keV is important. The uncertainty of this resonance strength of more than two orders of magnitude originated predominantly from the missing knowledge of the value of the transferred orbital angular momentum. The ground state of  $^{22}\text{Na}$  has spin-parity  $3^+$  and the  $E_x=7643$  keV state in  $^{23}\text{Mg}$  has, according to Endt [6], spin-parity  $3/2^+$  or  $5/2^+$ . An assignment of  $3/2^+$  would allow an orbital angular momentum transfer of  $l_{trans}=2$  only, whereas an  $5/2^+$  assignment allows both  $l_{trans}=0$  and  $l_{trans}=2$ . The transfer angular distribution of Ref. [3] had the shape of  $l_{trans}=2$ , however, does not allow to exclude the presence of an additional, small  $l_{trans}=0$  transfer cross section, which would add incoherently.

In a recent paper, [9, 10], Jenkins *et al.* have established, that the  $7643$  keV level has spin  $3/2^+$ . The experiment used the heavy ion fusion reaction  $^{12}\text{C}(^{12}\text{C}, n)^{23}\text{Mg}$  with a subsequent measurement of the radiative decay branches. The decay of the  $7643$  keV state by a measured  $7196$  keV  $\gamma$  ray to the first  $5/2^+$  excited state supported

\*Electronic address: comisel@venus.nipne.ro

arguments for the  $3/2^+$  spin assignment. Similar arguments fixed the spin assignment of the second 7622 keV state, which was also largely uncertain, to  $9/2^+$ . It is the purpose of this paper to give complementary arguments from a different, namely a shell model, approach in favor of a  $3/2^+$  assignment for the third state, and excluding a  $5/2^+$  assignment.

In this paper, we apply the Shell Model (SM) to calculate excitations in the mirror nuclei  $^{23}\text{Na}$  and  $^{23}\text{Mg}$ . We perform calculations of Thomas-Ehrman shifts to relate the levels of the two mirror nuclei and we compare the calculated properties of the levels with all available experimental information in order to relate the experimentally observed states with the calculated ones. The identification of a SM state with the  $E_x=7643$  keV state in  $^{23}\text{Mg}$  then fixes its spin.

While shell model calculations were applied usually to low lying excitations, they have been used successfully in the last decade to obtain also predictions for threshold states of astrophysical interest in the Ne-Na and Mg-Al stellar cycles, see *e.g.* the studies of Champagne *et al.* [7] and Iliadis *et al.* [8]. In the present work, based

only on the SM and Thomas-Ehrman shift calculations, we obtain results consistent with the results of Jenkins *et al.*, *i.e.* the same spin assignment for the 7643 keV level in  $^{23}\text{Mg}$ . We consider this as an argument in favor of an approach where shell model and Thomas-Ehrman shift calculations are extended to energies for high lying proton threshold states of astrophysical interest. This is the aim of the present work.

Fig. 1 shows the mirror levels in  $^{23}\text{Na}$  and  $^{23}\text{Mg}$  above the proton capture threshold in  $^{23}\text{Mg}$ . In our approach we start with SM calculations of  $^{23}\text{Na}$  since, in a fixed basis, these are known to describe better the levels of the neutron rich than the proton rich, less bound nucleus [7]. In addition, some levels are better known for  $^{23}\text{Na}$ . To compare the mirror levels of  $^{23}\text{Na}$  and  $^{23}\text{Mg}$  nuclei we take into account the corresponding Coulomb and Thomas-Ehrman shifts. The theoretical method for the calculation of the Coulomb shift of the energy of a level is discussed in section II. In section III this method is applied to the isobar analogue mirror states of  $^{23}\text{Na}$  and  $^{23}\text{Mg}$ . SM assignments for some of the  $^{23}\text{Mg}$  proton capture states are obtained and discussed. In section IV the astrophysical reaction rates are reevaluated and a temperature interval, limiting the hot and cold burning modes of a novae-supernovae scenario, is obtained.

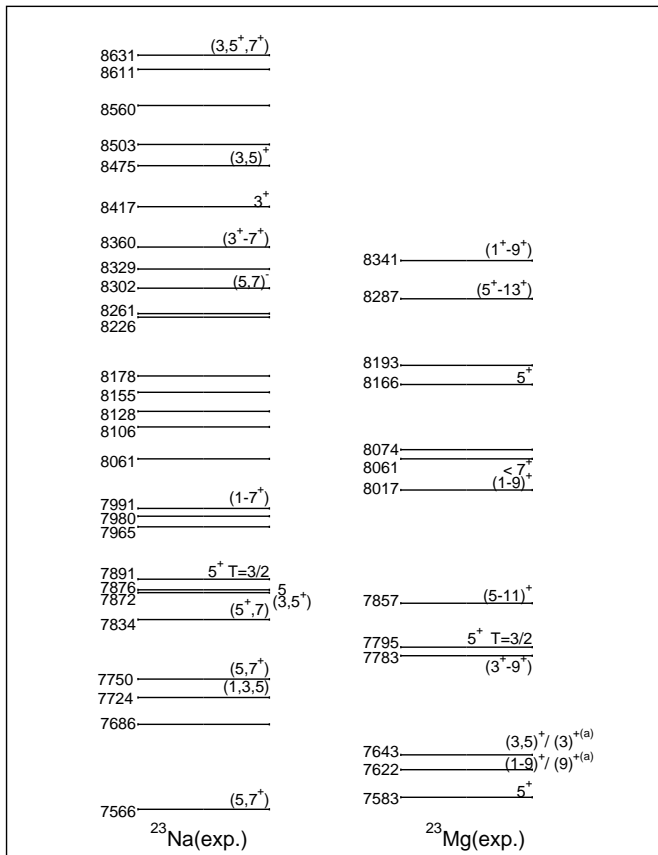


Figure 1: Excitation spectrum in  $^{23}\text{Na}$  and  $^{23}\text{Mg}$ , showing experimental data from Ref. [6], in the range of astrophysically interesting excitation energies above proton emission threshold in  $^{23}\text{Mg}$  ( $Q_p=7579$  keV). Spins are denoted by  $2J$ . <sup>(a)</sup> Recent spin assignments from Ref. [9].

## II. COULOMB AND THOMAS-EHRMAN SHIFTS IN MIRROR NUCLEI

The excited states in the mirror nuclei  $^{23}\text{Na}$  and  $^{23}\text{Mg}$  are isobaric analog states, the  $T_z=+1/2$  and  $T_z=-1/2$  members of an isospin  $T=1/2$  doublet. Thus from the knowledge of states of  $^{23}\text{Na}$  one may identify the states of interest in  $^{23}\text{Mg}$ . Because of the Coulomb repulsion, the latter ones are less bound. The positive parity states, we are considering here, had been calculated with the shell model code OXBASH [11] in the  $sd$  configuration space. These calculations go back to Wildenthal and use an established set of matrix elements [12]. This procedure is appropriate for well bound single particle configurations and reproduces many features of  $sd$ -shell nuclei in this mass range. Because of the fixed basis set of single particle wave functions, implied in the determination of the matrix elements, this procedure is more appropriate for the study of states in  $^{23}\text{Na}$  than for the less bound ones in  $^{23}\text{Mg}$ . For the states in  $^{23}\text{Mg}$  we assume the same configurations, as obtained for  $^{23}\text{Na}$ . To determine their excitation energies we calculate Coulomb shifts from a charge-dependent, isospin-nonconserving interaction (INC) [13] and in addition the Thomas-Ehrman shifts [14]. The latter ones take into account, that the proton single particle wave functions, in particular the  $2s1/2$  level, is spatially rather extended because of its low binding energy and the absence of a centrifugal barrier. Depending on the binding energy and spatial extension this leads to a reduction of the Coulomb interaction.

More precisely, the Coulomb shifts have been deter-

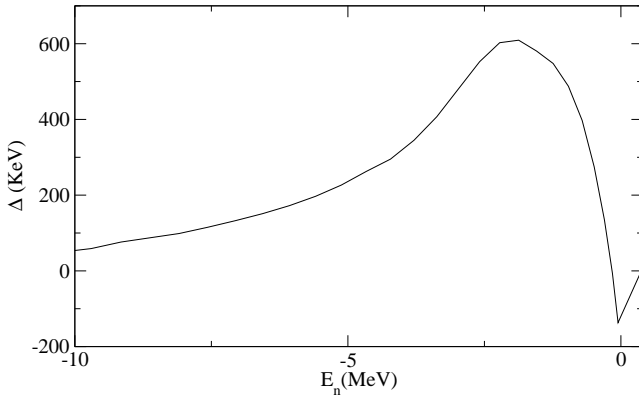


Figure 2: Calculated Thomas-Ehrman shift assuming pure  $2s1/2$  and  $1d5/2$  single particle states for  $A=23$  as a function of the  $s$ -wave neutron energy.

mined applying the method developed by Herndl *et al.* [15]. It uses the INC interaction and reproduces well the energy shifts between states of predominant  $d5/2$  or  $d3/2$  configurations. The Thomas-Ehrman shift [14] is derived from calculations with wave functions generated in a Woods-Saxon single particle potential model [16, 17]. Tombrello [18] first demonstrated that a one-body potential model with Coulomb interaction can describe the Thomas-Ehrman shift. For these calculations the shell model wave functions are considered as a sum of terms, where the valence nucleon is coupled to excited states of  $^{22}\text{Na}$ . Then the Thomas-Ehrman shift is determined from the calculated relative shifts of  $1d5/2$  and  $2s1/2$  proton versus neutron valence wave functions at single particle energies, given by the difference between the energy of the actual state and the excitation energy of the core state. In the summation the spectroscopic coefficients determine the weighting factors.

Using the Q-values from Ref. [5], the well depth of the Woods-Saxon potential is chosen to reproduce the single particle energies in the neutron rich isotope,  $^{23}\text{Na}$ . To determine the energy of the  $^{23}\text{Mg}$  mirror levels the same potential is used adding an extra Coulomb field of a uniform spherical charge of radius  $r_0 A^{1/3}$ . To take into account single particle states built onto excited cores,  $s$ -wave neutron and proton single particle orbits are considered for each of the states of  $^{22}\text{Na}$  core. The relative Thomas-Ehrman shift with respect to a pure  $1d5/2$  state is then determined as,  $\Delta\epsilon_{TE} = \Delta\epsilon_p - \Delta\epsilon_n$ , where  $\Delta\epsilon_{n(p)}$  are the single particle energy differences between  $1d5/2$  and  $2s1/2$  neutron (proton) single particle states. We have used a central Woods-Saxon potential with conventional values of the radius ( $r_0=1.25$  fm) and diffuseness (0.65 fm) and a uniform charge distribution ( $r_C=1.25$  fm).

The Thomas-Ehrman single particle shifts  $\Delta\epsilon_{TE}$  for the mirror levels of  $^{23}\text{Na}$  and  $^{23}\text{Mg}$  nuclei are a function of the  $2s1/2$  neutron single particle energy. This dependence is shown in Fig. 2. The Thomas-Ehrman shift falls to zero for higher excitation energies when the  $s$ -wave neutrons reach the threshold. A similar dependence has

been obtained for  $A=13$  mass region by Barker [19].

The energy range we have considered in the calculation of the TE shifts, shown in Fig. 2, is applicable for states of the  $^{22}\text{Na}$  core up to the ( $E_x=4360$  keV,  $J^\pi = 2^+$ ) level. As an example, the level (7750,  $(5/2^+, 7/2^+)$ ) in  $^{23}\text{Na}$  includes configurations of a  $s$ -wave neutron coupled to the ground state ( $0., 3^+$ ) as well as to the following excited states in  $^{22}\text{Na}$ : (1951,  $2^+(T=1)$ ), (1983,  $3^+$ ), (2968,  $3^+$ ), (3590,  $2^+$ ) and (4360,  $2^+$ ). The excitation energy, spin and parity for a nuclear level are denoted here and in what follows by ( $E_x$  (keV),  $J^\pi$ ). The  $s$ -wave neutron single particle energies determined from the Q-values and the excitation energies of the core are in the ( $-4670$ ,  $-310$ ) keV range. This interval covers the significant contributions to the Thomas-Ehrman shift, see Fig. 2.

The resulting relative single particle shifts are multiplied by the corresponding  $2s1/2$  spectroscopic coefficients from the SM calculation. This term is then summed with the SM Coulomb shift using the INC interaction, yielding the total energy displacement. Finally, this quantity will be added to an experimental level in  $^{23}\text{Na}$  with known spin-parity assignment, to obtain the predicted isobar analogue state in the proton-rich nucleus  $^{23}\text{Mg}$ .

### III. SHELL MODEL CALCULATIONS AND OBSERVED EXCITED STATES

For the mirror nuclei  $^{23}\text{Na}$  and  $^{23}\text{Mg}$  we have reliable assignments for the levels up to 5778 keV in  $^{23}\text{Na}$  and 5711 keV in  $^{23}\text{Mg}$  (*e.g.* Table 23j from Ref. [6]). In Table I we show the quality of the Coulomb shift calculations of these low lying bound levels, from which we also obtain an estimate of the accuracy of the predictions. The first columns list the low lying states in  $^{23}\text{Na}$  and their calculated and experimental excitation energies. In the following columns we relate this to the experimental energies and predicted values  $E_x^{TES}$  for the mirror nucleus  $^{23}\text{Mg}$ . The last column gives the difference of these two quantities. The observed mean deviation is about  $\pm 60$  keV, the largest observed one is 138 keV. From this we assume, that in the region of the proton capture states in  $^{23}\text{Mg}$  the calculated energies of the Coulomb shifted SM states and the experimentally observed ones should have twice this mean deviation, that is  $\pm 120$  keV, *see e.g.* the methods used in Ref. [7] or Ref. [8].

As discussed in the introduction the states of interest for the astrophysical question of the Ne-Na cycle are the above threshold resonances in  $^{23}\text{Mg}$ , in particular the second and third state, whose spin assignments were uncertain before the work of Ref. [9, 10]. The aim is to make a correspondence between these states and the shell model levels. In Table II we list for the first three states above threshold in  $^{23}\text{Mg}$  those SM states, whose spin assignments and Coulomb shifted energies fall into the experimental range of spins and the  $\pm 120$  keV en-

Table I: Experimental and shell model positive parity states in  $^{23}\text{Na}$  and  $^{23}\text{Mg}$  below the proton threshold. For  $^{23}\text{Na}$  we give the experimental energy  $E_{\text{x}}$ (keV) and spin assignment  $2J^{\pi}$  and the corresponding shell model states  $2J_{SM}^{\pi}$  and the energies including the INC interaction  $E_{\text{x}}^{INC}$ . For  $^{23}\text{Mg}$  this is put in correspondence with the experimental analogue states and energies. We further show the energies predicted from the Coulomb shift calculations  $E_{\text{x}}^{TES}$ , which are obtained from the relation:  $E_{\text{x}}^{TES} = E_{\text{x}}(^{23}\text{Na}) + \Delta E_C - \Delta E_{TE}$ , where  $\Delta E_C = E_{\text{x}}^{INC}(^{23}\text{Mg}) - E_{\text{x}}^{INC}(^{23}\text{Na})$  is the pure Coulomb shift and  $\Delta E_{TE} = \sum C^2 S(2s1/2) \Delta \epsilon_{TE}$  is the Thomas-Ehrman shift (see section II). The last column gives the difference between the experimental and predicted energies for  $^{23}\text{Mg}$ .

$2J_{SM}^{\pi}$	$^{23}\text{Na}$			$^{23}\text{Mg}$			$\Delta E_{\text{x}}^b$
	$2J^{\pi a}$	$E_{\text{x}}^{INC}$	$E_{\text{x}}^a$	$2J^{\pi a}$	$E_{\text{x}}^{TES}$	$E_{\text{x}}^a$	
3 <sub>1</sub> <sup>+</sup>	3 <sup>+</sup>	0	0	3 <sup>+</sup>	0	0	+34
5 <sub>1</sub> <sup>+</sup>	5 <sup>+</sup>	411	440	5 <sup>+</sup>	417	451	+79
7 <sub>1</sub> <sup>+</sup>	7 <sup>+</sup>	2119	2076	7 <sup>+</sup>	1972	2051	+61
1 <sub>1</sub> <sup>+</sup>	1 <sup>+</sup>	2297	2391	1 <sup>+</sup>	2297	2359	+81
9 <sub>1</sub> <sup>+</sup>	9 <sup>+</sup>	2785	2704	9 <sup>+(5+)</sup>	2633	2715	+138
3 <sub>2</sub> <sup>+</sup>	3 <sup>+</sup>	2730	2982	(3, 5) <sup>+</sup>	2917	2908	-8
5 <sub>2</sub> <sup>+</sup>	5 <sup>+</sup>	3853	3914	(3, 5) <sup>+</sup>	3726	3864	+138
1 <sub>2</sub> <sup>+</sup>	1 <sup>+</sup>	4289	4430	1 <sup>+</sup>	4397	4354	-43
7 <sub>2</sub> <sup>+</sup>	7 <sup>+</sup>	4615	4775	(1 - 9) <sup>+</sup>	4695	4685	-10
5 <sub>3</sub> <sup>+</sup>	5 <sup>+</sup>	5221	5379	(3, 5) <sup>+</sup>	5327	5287	-40
11 <sub>1</sub> <sup>+</sup>	11 <sup>+</sup>	5365	5534	$\geq 3^+$	5420	5456	+36
5 <sub>4</sub> <sup>+</sup>	5 <sup>+</sup>	5529	5742	5 <sup>+</sup>	5713	5656	-57
3 <sub>3</sub> <sup>+</sup>	3 <sup>+</sup>	5724	5766	(1 - 9) <sup>+</sup>	5694	5691	-3
9 <sub>2</sub> <sup>+</sup>		5948	5778	(1 - 9) <sup>+</sup>	5626	5711	+85

<sup>a</sup>Experimental data from Ref. [6].

<sup>b</sup> $\Delta E_{\text{x}}$ (keV)= $E_{\text{x}}(^{23}\text{Mg}) - E_{\text{x}}^{TES}$

ergy interval of the experimental energy. These states then are possible candidates to be assigned to the experimental proton resonances of  $^{23}\text{Mg}$ . It is seen that this choice is rather wide for the second state at 7622 keV and still contains four candidates for the 7643 keV state, which is of main interest here. The determination of the spins of these two levels by Ref. [9], of course, limits these numbers considerably. We also list the resonance strength  $\omega\gamma$  of these SM states. We also note, that the only known  $T=3/2$  isobar analogue state above proton threshold, the  $J^{\pi}=5/2^+$ , 7795 keV state, is identified reasonably well with the  $5/2_9^+$  SM state at 7760 keV (not shown in Table II).

We now want to determine from the SM point of view whether the third proton capture resonance state at  $E_{\text{x}}=7643$  keV has  $J^{\pi}=3/2^+$  or  $5/2^+$ . As shown in Table II we have to consider the positive parity SM states  $J^{\pi}=3/2_6^+, 3/2_7^+, 5/2_8^+$  and  $5/2_{10}^+$ , since, as noted above, the  $5/2_9^+$  SM state is already identified with the  $T=3/2$  isobar analogue state above proton threshold. To do so we want to argue that we can exclude the two other  $5/2^+$  states, because they have to be assigned to two other states. The first resonance state at  $E_{\text{x}}=7583$  keV has spin  $5/2^+$ ; thus we identify this state with the  $5/2_8$  SM state. Now it remains to identify a higher excited state

Table II: Possible shell model assignations for the first three threshold states in  $^{23}\text{Mg}$ . Their resonance strengths were calculated (see section IV) by using SM spectroscopic factors.

$E_{\text{x}}^a$	$2J^{\pi a}$	$2J_{SM}^+$	$\omega\gamma$ (meV)
7583	5 <sup>+</sup>	5 <sub>8</sub> 5 <sub>10</sub>	$2.3 \times 10^{-71}$ 4.7 $\times 10^{-71}$
7622	(1 - 9) <sup>+</sup>	1 <sub>4</sub> 1 <sub>5</sub> 3 <sub>6</sub> 3 <sub>7</sub> 5 <sub>8</sub> 5 <sub>10</sub> 7 <sub>6</sub> 7 <sub>7</sub> 9 <sub>7</sub>	$1.6 \times 10^{-16}$ 4.9 $\times 10^{-15}$ $1.0 \times 10^{-15}$ 5.6 $\times 10^{-15}$ $1.1 \times 10^{-12}$ 2.5 $\times 10^{-12}$ $7.2 \times 10^{-12}$ 5.4 $\times 10^{-13}$ $4.0 \times 10^{-14}$
7643	(3, 5) <sup>+</sup>	3 <sub>6</sub> 3 <sub>7</sub> 5 <sub>8</sub> 5 <sub>10</sub>	$1.3 \times 10^{-11}$ 7.2 $\times 10^{-11}$ $1.4 \times 10^{-8}$ 3.1 $\times 10^{-8}$

<sup>a</sup>Experimental data from Ref. [6].

as the  $5/2_{10}^+$ . As seen in Fig. 1, at higher experimental excitation energies in  $^{23}\text{Na}$  there are two neighboring states with known and restricted spin and parities:  $(8417, 3/2^+)$  and  $(8475, (3/2, 5/2)^+)$ . According to the above procedure the SM calculation relates these levels in  $^{23}\text{Na}$  to  $(8417, 3/2_7^+)$  and to  $(8475, 3/2_7^+ \text{ or } 5/2_{11}^+)$ , respectively. Because of the mutual exclusion we assign the 8475 keV level as  $5/2_{11}^+$ . Applying the shift procedure, the  $5/2^+$  mirror state in  $^{23}\text{Mg}$  is predicted at  $E_{\text{x}}=8302$  keV. This excitation energy exceeds the energy of the known  $(8166, 5/2^+)$  level in  $^{23}\text{Mg}$  by 136 keV; thus outside our energy interval. Thus we have to identify the  $(8166, 5/2^+)$  experimental level as the  $5/2_{10}^+$  SM state. We will come back to this state below. Thus the  $J^{\pi}=5/2_8^+, 5/2_9^+$  and  $5/2_{10}^+$  SM states have all been assigned. It follows that the  $J^{\pi}=3/2^+$  state corresponds to the 7643 keV level.

To further support the spin assignments in this energy range, a comparison between the theoretical and available experimental data for spectroscopic factors, Gamow-Teller  $\beta$  decay strengths, M1 transition probabilities, and gamma-branching ratios are discussed in the following.

### a) Spectroscopic coefficients.

First we compare SM with experimental single proton transfer spectroscopic factors from Schmidt *et al.* [3]. The calculated SM spectroscopic factor  $(2J+1)C^2 S=0.02$  for the  $3/2_6^+$  state is considerably smaller than the value of  $(2J+1)C^2 S=0.10$  for the  $3/2_7^+$  state. The experimental value for the 7643 keV level is  $(2J+1)C^2 S=0.34$  ( $l=2$ ) (see Ref. [3], Table 3.)

### b) Gamow-Teller $\beta$ decay transitions.

In a recent paper of Fujita *et al.* [21] the GT transition strengths for  $^{23}\text{Mg} \rightarrow ^{23}\text{Na}$   $\beta$  decay has been determined, analyzing the  $^{23}\text{Na}(^3\text{He}, t) ^{23}\text{Mg}$  reaction. The results are shown in Table III together with the SM transition strengths  $B(\text{GT})$  computed with the OXBASH code. The SM values are systematically too large, reproduce, however, the trend of the data. The experimental  $B(\text{GT})$  for the  $(8166, 5/2^+)$  level in  $^{23}\text{Mg}$  is  $0.29 \pm 0.015$  while

Table III: The experimental and theoretical values for: GT transition strengths  $B(GT)$  corresponding to the  $^{23}\text{Mg} \rightarrow ^{23}\text{Na}$   $\beta$  decay and M1 transition strengths  $B(\text{M1})\uparrow$  (units of  $\mu_N^2$ ).

States in $^{23}\text{Mg}$			$B(\text{GT})$		States in $^{23}\text{Na}$			$B(\text{M1})\uparrow$	
$E_x^a$	$2J^\pi$	Experimental <sup>b</sup>	Experimental <sup>b</sup>	Theoretical <sup>c</sup>	$E_x^a$	$2J^\pi$	Experimental <sup>d</sup>	Experimental <sup>d</sup>	Theoretical <sup>c</sup>
0	$3^+$	$0.340 \pm 0.014$		0.541	440	$5^+$	$0.554 \pm 0.034$		0.483
451	$5^+$	$0.146 \pm 0.006$		0.409	2391	$1^+$	$0.0017 \pm 0.0003$		0.026
2359	$1^+$	$0.055 \pm 0.004$		0.199	2982	$3^+$	$0.292 \pm 0.041$		0.304
2908	$(3, 5)^+$	$0.193 \pm 0.011$		0.574	3914	$5^+$	$0.090 \pm 0.015$		0.065
3864	$(3, 5)^+$	$0.055 \pm 0.004$		0.146	4430	$1^+$	$1.02 \pm 0.07$		0.877
4354	$1^+$	$0.250 \pm 0.013$		0.717	5379	$5^+$	$0.33 \pm 0.12$		0.199
5287	$(3, 5)^+$	$0.066 \pm 0.005$		0.186	5742	$5^+$	$0.66 \pm 0.04$		0.327
8166	$5^+$	$0.290 \pm 0.015$	$(5_{10})^e$	0.312	5766	$3^+$	$0.25 \pm 0.04$		0.238
			$(5_{11})^e$	0.058	7133	$(3, 5)^+$	$0.31 \pm 0.07$		0.464
					8360	$(3^+ - 7^+)$	$0.290 \pm 0.13$	$(3_7)^e$	0.032
								$(5_{10})^e$	0.221
								$(5_{11})^e$	0.064
					8830	$1^+$	$0.050 \pm 0.022$		0.067

<sup>a</sup>Experimental data from Ref. [6].

<sup>b</sup>From Ref. [21].

<sup>c</sup>Using W interaction.

<sup>d</sup>From Ref. [21], [6].

<sup>e</sup>2J (SM) spins accordingly with *sdpn* model space.

Table IV: Experimental gamma ray branching ratio (%) to the ground state and the first two excited levels for the states,  $E_x=8360$  keV,  $J^\pi=(3/2^+ - 7/2^+)$  and  $E_x=8166$  keV,  $J^\pi=5/2^+$  in  $^{23}\text{Na}$  and  $^{23}\text{Mg}$ , respectively, (energies in keV). The values corresponding to another possible mirror state in  $^{23}\text{Na}$  nucleus,  $E_x=8475$  keV,  $J^\pi=(3/2 - 5/2)^+$  are also listed.

$E_x$	States in $^{23}\text{Na}$ <sup>a</sup>			States in $^{23}\text{Mg}$ <sup>b</sup>		
	$2J^\pi$	8360	8475	$E_x$	$2J^\pi$	8166
0.0	$3^+$	$53 \pm 3$		0.0	$3^+$	$65 \pm 5$
440	$5^+$	$32 \pm 3$	(50)	451	$5^+$	$19 \pm 2$
2076	$7^+$	$15 \pm 2$		2051	$7^+$	$16 \pm 2$
other levels			(50)			
			unknown			

<sup>a</sup> Exp. gamma ray branching ratios from Ref. [6].

<sup>b</sup> Exp. gamma ray branching ratios from Ref. [2].

the predictions for the  $J^\pi=5/2_{10}^+$  and  $5/2_{11}^+$  SM states are 0.312 and 0.058 respectively. This observation nicely supports the  $J^\pi=5/2_{10}^+$  SM assignment, discussed above.

### c) M1 gamma transitions.

The M1 transition strengths  $B(\text{M1})\uparrow$  from the ground to the excited states in  $^{23}\text{Na}$  are calculated from the SM transition densities and are compared to the experimental ones of Fujita *et al.* [21], and are also shown in Table III. The theoretical and experimental values generally are in good agreement. In particular, the experimental value of ( $B(\text{M1})=0.290 \pm 0.13$ ) for the  $E_x=8360$  keV in  $^{23}\text{Na}$  agrees well with ( $B(\text{M1})=0.221$ ) for the  $5_{10}^+$  SM state. This then supports the  $5/2_{10}^+$  SM assignment for the  $E_x=8166$  keV excited state in  $^{23}\text{Mg}$ , as discussed. The predicted excitation energy of the

Table V: Experimental and Shell Model  $5/2^+$  states in  $^{23}\text{Mg}$ . The  $E_x^{TES}$  predicted energies written in brackets were obtained from assumed assignments of the analogue states in  $^{23}\text{Na}$ .

$2J_{SM}^\pi$	$2J^\pi$	$E_x^a$	$E_x^{TES}$	$\Delta E_x^b$
$5_1^+$	$5^+$	451	417	+34
$5_2^+$	$(3, 5)^+$	3864	3726	+138
$5_3^+$	$(3, 5)^+$	5287	5327	-40
$5_4^+$	$5^+$	5656	5713	-57
$5_5^+$	$5^+$	6568	(6632)	(-64)
$5_6^+$	$5^+$	6899	(6856;6906)	(43;-7)
$5_7^+$	$5^+$	6984	(6950)	(+44)
$5_8^+$	$5^+$	7583	7466 to 7702	
$5_9^+$	$5^+, T=3/2$	7795	7760	+35
$5_{10}^+$	$5^+$	8166	8100	+66
$5_{11}^+$		8193 to 8420	8302	

<sup>a</sup>Experimental data from Ref. [6].

<sup>b</sup>  $\Delta E_x(\text{keV})=E_x(^{23}\text{Mg}) - E_x^{TES}$

mirror state in  $^{23}\text{Mg}$  exceeds the experimental one by  $\Delta E_x \simeq 70$  keV only.

### d) Gamma-branching ratios.

The mirror relation of the  $E_x=8360$  keV state in  $^{23}\text{Na}$  and the  $E_x=8166$  keV state in  $^{23}\text{Mg}$  is further supported by the experimental gamma branching ratios to low lying state in these nuclei. This is shown in Table IV together with data from the literature. The agreement is surprisingly good. In contrast, another candidate analogue state in  $^{23}\text{Na}$  at  $E_x=8475$  keV has appreciable deviations.

Summarizing the arguments (a)-(d), the present analysis further supports the  $5_{10}^+$  SM assignment to the

Table VI: The resonance strengths for the three lowest states in  $^{23}\text{Mg}$  above the proton threshold.

$E_x(\text{keV})^a$	$2J^\pi$	$\omega\gamma(\text{meV})^b$			
		Ref. [3]		Ref. [10]	Present high
		low	high		
7583	$5^+$	0	$1.3 \times 10^{-63}$		
7622	$(1-9)^+$	$5.6 \times 10^{-14}$	$8.8 \times 10^{-12}$	$1.7_{-1.1}^{+2.5} \times 10^{-13}$	$1.0 \times 10^{-13}^c$
7643	$(3-5)^+$	$1.2 \times 10^{-10}$	$3.1 \times 10^{-8}$	$2.2_{-1.4}^{+3.0} \times 10^{-9}$	$2.2 \times 10^{-10}$

<sup>a</sup>From Ref. [6].

<sup>b</sup>According to the spin assignments and resonance energies used in the cited works.

<sup>c</sup>According to the spin assignment of Ref. [10].

$E_x=8166$  keV state in  $^{23}\text{Mg}$ . This in turn supports the  $J^\pi=3/2^+$  assignment of the 7643 keV level. We thus see that purely from SM arguments we are able to assign a spin to the 7643 keV level in  $^{23}\text{Mg}$ . At similar argument would be more difficult with the second 7622 keV level, because of many SM possibilities listed in Table II.

From the above arguments we are able to assign the first ten  $5/2^+$  states in the SM calculations to definite states in  $^{23}\text{Mg}$ . This is shown in Table V for all the states up to about 8 MeV excitation energy. One can also make some spin assignments more definite. The second and third states of  $^{23}\text{Mg}$  at  $E_x=3864$  and 5287 keV are IAR of the states at  $E_x=3914$  and 5379 keV in  $^{23}\text{Na}$  [6] with spins  $5/2^+$ . Consequently these two states of  $^{23}\text{Mg}$  are also  $5/2^+$  states. All other higher states from Table V have a well-assigned  $5/2^+$  spin; there is no place for assignment of  $5/2^+$  spin to the 7643 level in  $^{23}\text{Mg}$ , lending further support to the assignment of  $3/2^+$ . In addition this table demonstrates that SM calculations can be useful to identify experimental levels also at excitation energies above the threshold, and can thus be of use in astrophysical considerations.

#### IV. RESONANCE STRENGTHS AND STELLAR REACTION RATES

The resonance strengths for the states just above the proton threshold has been determined by the relation,

$$\omega\gamma = \frac{2J+1}{2(2J_0+1)} \frac{\Gamma_p \Gamma_\gamma}{\Gamma_{tot}} \approx \frac{2J+1}{2(2J_0+1)} \Gamma_p$$

where  $J_0$  is the spin of  $^{22}\text{Na}$  target,  $J$  is the spin of the resonant state, while  $\Gamma_p$ ,  $\Gamma_\gamma$  and  $\Gamma_{tot}$  are the partial proton width in the entrance channel, the partial  $\gamma$  width in the exit channel and the total width, respectively. The last equality is valid for  $\Gamma_\gamma \ll \Gamma_p$ , as here. The proton widths are determined as product of the spectroscopic factors (from SM calculations or from experimental data) and the single particle width  $\Gamma_p = C^2 S \times \Gamma_{sp}$ , where  $C$  is the isospin Clebsch-Gordan coefficient. The single particle width is derived within the optical model as a product of the penetration factor and the Wigner unit

$\Gamma_{sp} = P|u(r_a)|^2$  [20]. The same parameters of the optical potential have been used, as for the Thomas-Ehrman shift evaluation.

The experimental information on the lowest three states in  $^{23}\text{Mg}$  above the proton threshold which have been included in the calculation of the reaction rate is shown in Table VI. The excitation energies and the knowledge about the spin-parities  $J^\pi$  are given in columns 1 and 2, accordingly with Ref. [6]. The remaining columns give the experimental information on the resonance strength. In column 3 and 4 we give the low and high limits of Ref. [3] (which includes the uncertainty due to the uncertainty of the spin of the second and third states), and in column 5 the values quoted by Jenkins *et al.* in their last publication [10]. In the last column the results for the higher limits of the present work are given. The lower limits are nearly the same as the lower ones from Ref. [3] and we did not list them again in Table VI. The low and high limits of the resonance strengths from Ref. [3] for the third level were mainly due to the possible  $l=2$  and  $l=0$  values of the transferred orbital momenta. The elimination of  $l=0$  orbital now reduces strongly the range of possible values of the resonance strength. Using the experimental spectroscopic coefficient for  $l=2$  and the prescription from Ref. [3] for the upper limit of  $\omega\gamma$ , the maximum value of the resonant strength is now  $\omega\gamma(\text{expt.})_{high} = 2.2 \times 10^{-10}$  meV.

Of particular interest is the strength of the third state. While the limits for the strength in Refs. [3, 4] are almost the same and rather wide, these are quite narrowly defined in the present work. The values quoted in Refs. [9] and [10] are different. In the table and in the ensuing calculations we have used the latest values which are considerably higher than those of the present work, even though now the same spin assignment is used.

The astrophysical reaction rates have been computed according to the formalism of narrow resonances [22], where the contributions are calculated separately for each of the analyzed levels. The resonant reaction rates depend on the resonance energies  $E_r$  and the resonance strengths  $\omega\gamma$ , as well as on the  $T_9$  temperature, [23],

$$N_A < \sigma v >_r = 1.54 \times 10^{11} (AT_9)^{-3/2} (\omega\gamma) \exp\left(-\frac{11.605 E_r}{T_9}\right)$$

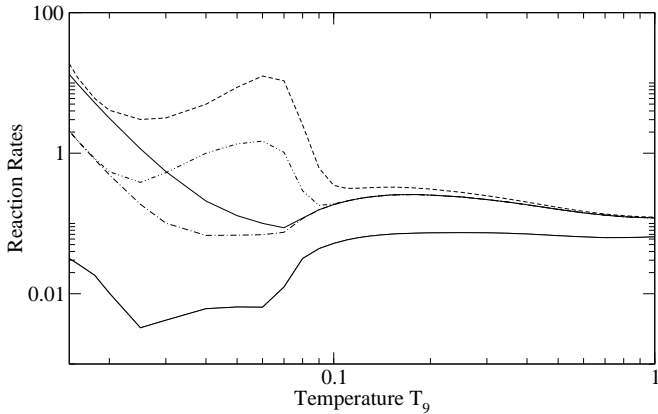


Figure 3: Upper and lower limits of the reaction rate versus stellar temperature  $T_9$  for the  $^{22}\text{Na}(p, \gamma)^{23}\text{Mg}$  reaction. Using the adopted values of Ref. [4] the lower solid and the upper dashed curves are obtained. We also show the modifications of the upper limit of the reaction rate due other assumptions. The upper solid line is the reaction rate of this work taking into account the  $3/2^+$  spin assignment of the third level. The dash-dotted curve is obtained from this solid curve by using for the second state the spin assignment given by Ref. [10]. The dash-double-dotted curve uses in addition the strength of the third state as given in Ref. [10]. The reaction rates are normalized to those of Caughlan and Fowler, Ref. [24].

Here,  $A$  is the reduced mass,  $A = A_p A_T / (A_p + A_T)$ ,  $A_p$  is the projectile mass, and  $A_T$  is the target mass. The reaction rate  $N_A < \sigma v >_r$  is expressed in units of  $\text{cm}^3 \text{s}^{-1} \text{mol}^{-1}$  if the strengths are given in meV, the resonance energies in MeV, and temperatures  $T_9$  in  $10^9 \text{K}$ .

In Fig. 3 the upper and lower limits of the reaction rate with the various assumptions are shown, normalized to the ones calculated by Caughlan and Fowler, Ref. [24]. The lower solid line and the highest dashed lines correspond to the reaction rate obtained with the lower and upper values, respectively, for the strength functions adopted by Ref. [4]. The other curves represent the upper limits with the other assumptions. The upper solid line is the reaction rate of this work taking into account the spin  $3/2^+$  assignment of the third level. The dash-dotted curve is obtained from this solid curve by using for the second state the spin assignment of Ref. [10] and corresponding spectroscopic factor of Ref. [3]. The dash-double-dotted curve uses in addition the strength of the third state as given in Ref. [10]. Two aspect will be noted: first, the upper limit of Jenkins *et al.*, is much higher, due to the higher resonance strength. Secondly, the more precise limits for the second state do not much affect the reaction rate in the astrophysically interesting region above  $T_9 > 0.05$ .

From the above limits of the reaction rates, the limits of the lifetime against proton capture  $\tau_p(^{22}\text{Na}) = (\rho X_H N_A < \sigma v >)^{-1}$  versus stellar temperature  $T_9$ , have been calculated assuming a stellar density of  $\rho = 1000 \text{g/cm}^3$  and a hydrogen mass fraction  $X_H = 1$ . These limits are compared to the  $\beta$ -decay lifetime  $\tau_\beta(^{22}\text{Na})$  in Fig. 4.

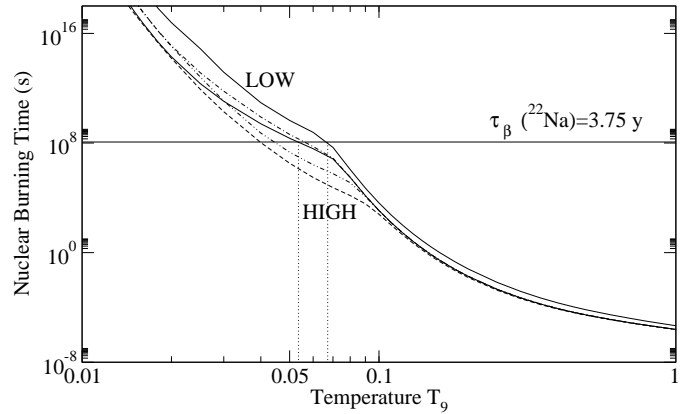


Figure 4: The  $\beta$ -decay lifetime  $\tau_\beta(^{22}\text{Na})$  and the limits of lifetime of  $^{22}\text{Na}$  against proton capture,  $\tau_p(^{22}\text{Na})$ , versus temperature, calculated for a pure hydrogen composition and a density of  $\rho = 1000 \text{ g/cm}^3$ . The curves were obtained from the reaction rates shown in Fig. 3.

The intersections with this line determine the limits of temperature corresponding to the cycle switches between cold and hot burning modes. The lines represent the different assumptions on the burning rates in Fig. 3, where the same line signatures are used as there, except, of course, that upper and lower limits are now interchanged. For the reaction rates of Ref. [4] (solid upper and dashed lower line) the limits  $T_9 = 0.039$  and  $T_9 = 0.068$  had already been calculated in Ref. [3]. Using the upper limit for the reaction rate of this work (solid lower line), the temperature interval defining the burning mode lies at  $T_9 = 0.055$  to  $T_9 = 0.068$  (marked by dotted vertical lines in Fig. 4), thus considerably sharpening the lower limit. Using instead the smaller values corresponding to the  $9/2^+$  spin assignment of Ref. [10] for the second resonance (dash-dotted line) does not significantly change the lower limit of the cycle switching temperature. Finally using the value of Ref. [10] for the third resonance strength (dash-double-dotted line) significantly lowers the lower limit.

## V. CONCLUSIONS

In view of the astrophysical importance of the  $^{22}\text{Na}(p, \gamma)^{23}\text{Mg}$  reaction, we have analyzed the spin and parity of the lowest levels above the proton capture threshold in the  $^{23}\text{Mg}$  nucleus with the help of Shell Model calculations. The predicted SM levels for the mirror nuclei  $^{23}\text{Na}$  and  $^{23}\text{Mg}$  were calculated using the Wildenthal interaction in the appropriate  $sd$  space model. The isobar analogue nuclear levels were matched theoretically by calculating the Coulomb displacements, including the Thomas-Ehrman shifts.

From the comparison of the SM and experimental energy levels and other spectroscopic data, in particular spectroscopic coefficients, Gamow Teller beta decay and  $B(\text{M1})$  gamma transition amplitudes and experimental

gamma-branching ratios, we deduced that the third state just above the proton threshold in  $^{23}\text{Mg}$  at  $E_x=7643$  keV has a  $3/2^+$  spin assignment. This is in agreement with dedicated experimental studies by Jenkins *et al.* [9, 10], who also argued for a  $3/2^+$  value. Their  $9/2^+$  spin assignment for the lower  $E_x=7622$  keV level, the second above threshold, cannot be uniquely predicted by the present SM approach. However it does not significantly contribute to the astrophysical reaction rate for  $T_9 > 0.05$  or for the expected lower limit of the cycle switching temperature. Using the lower limit of our resonance strength for the third, *i.e.*  $3/2^+$ , resonance above the proton threshold, we obtain significantly reduced upper limits for the thermonuclear reaction rate below  $T_9=0.1$ . Consequently, the temperature interval defining the stellar burning modes for a novae-supernovae scenario is accord-

ingly narrowed.

More generally, we have demonstrated the usefulness of SM calculations in obtaining assignments of high lying levels, even above threshold, which might be of interest in astrophysical reaction scenarios.

## Acknowledgments

C.H. acknowledges support of the A. von Humboldt-Stiftung and the hospitality at the Ludwig-Maximilians-University of Munich, while working on final variant of this work. H.C. acknowledges the hospitality of the Max-Planck-Institute for Extraterrestrial Physics (MPE) at Garching.

---

[1] D.C. Black, Geoch. Cosmoch. Acta **36**, 347 (1972).  
 [2] S. Seuthe, C. Rolfs, U. Schröder, W.H. Schulte, E. Somorjai, H.P. Trautvetter, F.B. Waanders, R.W. Kavanagh, H. Ravn, M. Arnould, G. Paulus, Nucl. Phys. **A514**, 471 (1990).  
 [3] S. Schmidt, C. Rolfs, W.H. Schulte, H.P. Trautvetter, R.W. Kavanagh, C. Hategan, S. Faber, B.D. Valnion, G. Graw, Nucl. Phys. **A591**, 227 (1995).  
 [4] C. Angulo, M. Arnould, M. Rayet, P. Descouvemont, D. Baye, C. Leclercq-Willain, A. Coc, S. Barhoumi, P. Aguer, C. Rolfs, R. Kunz, J.W. Hammer, A. Mayer, T. Paradellis, S. Kossionides, C. Chronidou, K. Spyrou, S. Degl'Innocenti, G. Fiorentini, B. Ricci, S. Zavatarelli, C. Providencia, H. Wolters, J. Soares, C. Grama, J. Rahighi, A. Shotter, M. Lamehi Rachti, Nucl. Phys. **A656**, 3 (1999).  
 [5] G. Audi, A.H. Wapstra, Nucl. Phys. **A595**, 409 (1995).  
 [6] P.M. Endt, Nucl. Phys. **A633**, 1 (1998); Nucl. Phys. **A521**, 1 (1990).  
 [7] A.E. Champagne, B.A. Brown, R. Scherr, Nucl. Phys. **A556**, 123 (1993).  
 [8] C. Iliadis, L. Buchmann, P.M. Endt, H. Herndl, M. Wiescher, Phys. Rev. C **53**, 475 (1996).  
 [9] D.G. Jenkins, C.J. Lister, R.V.F. Janssens, T.L. Khoo, E.F. Moore, K.E. Rehm, B. Truett, A.H. Wuosmaa, M. Freer, B.R. Fulton, J. Jose, Phys. Rev. Lett. **92**, 031101 (2004).  
 [10] D.G. Jenkins, C.J. Lister, R.V.F. Janssens, T.L. Khoo, E.F. Moore, K.E. Rehm, D. Seweryniak, A.H. Wuosmaa, T. Davinson, P.J. Woods, A. Jokinen, H. Penttila, G. Martinez-Pinedo, J. Jose, Eur. Phys. J. A **27**, 117-121 (2006);  
 D.G. Jenkins, B.R. Fulton, C.J. Lister, R.V.F. Janssens, T.L. Khoo, E.F. Moore, K.E. Rehm, B. Truett, A.H. Wuosmaa, M. Freer, J. Jose, Nucl. Phys. **A758**, 749c-752c (2005).  
 [11] B.A. Brown, A. Etchegoyen and W.D.M. Rae, The computer code OXBASH, MSU-NSCL Report No. 524.  
 [12] B.H. Wildenthal, Prog. Part. Nucl. Phys. **11**, 5 (1984).  
 [13] W.E. Ormand, B.A. Brown, Nucl. Phys. **A491**, 1 (1989); W.E. Ormand, Phys. Rev. C **55**, 2407 (1997).  
 [14] J.B. Ehrman, Phys. Rev. **81**, 412 (1951); R.G. Thomas, Phys. Rev. **88**, 1109 (1952), **81**, 148 (1951).  
 [15] H. Herndl, J. Görres, M. Wiescher, B.A. Brown, L. Van Wormer, Phys. Rev. C **52**, 1078 (1995).  
 [16] R. Sherr and G. Bertsch, Phys. Rev. C **32**, 1809 (1985).  
 [17] H.T. Fortune, Phys. Rev. C **52**, 2261 (1995).  
 [18] T.A. Tombrello, Phys. Lett. **23**, 134 (1966).  
 [19] F.C. Barker, Phys. Rev. C **53**, 2539 (1996).  
 [20] P.D. Kunz, computer code DWUCK 4, unpublished.  
 [21] Y. Fujita, Y. Shimbara, I. Hamamoto, T. Adachi, G.P.A. Berg, H. Fujimura, H. Fujita, J. Görres, K. Hara, K. Hatanaka, J. Kamiya, T. Kawabata, Y. Kitamura, Y. Shimizu, M. Uchida, H.P. Yoshida, M. Yoshifuku, M. Yosoi, Phys. Rev. C **66**, 044313 (2002).  
 [22] C.E. Rolfs and W.S. Rodney, Cauldrons in the Cosmos (University of Chicago Press, Chicago, 1988).  
 [23] W.A. Fowler, G.R. Caughlan and B.A. Zimmerman, Annu. Rev. Astro. Astrophys. **13**, 69 (1975).  
 [24] G.R. Caughlan and W.A. Fowler, At. Data Nucl. Data Tables **40**, 283 (1988).